Establishing New Procedures for Evaluating Landslide Vulnerability in Southern Taiwan by Multitemporal Images

Hern Wang[1], Kuan-Tsung Chang[2*], Chih-Ping Kuo[3], and Jin-King Liu[4]

Abstract: This paper proposed to use the archival images of the FORMOSAT-II satellite in the last 11 years to explore the high landslide vulnerability areas. The interpretation results will be published on a dedicated three-dimensional digital platform in the cloud. This study demonstrated how to performlong-term change for the landslide susceptibility using multi-temporal historical images. The analysis results can provide the allocation of high vulnerable sites for continuous monitoring and other value-added applications.

Keywords: Landslide, Satellite, Land, Digital Earth

1. Introduction

Landslides are a natural phenomenon for the dynamic bal-ance of the earth's surface. The potential or intrinsic factors of landslides include geological and morphological factors. The external or triggering factors include earthquakes, climate, hydrology, and human activities. In Taiwan, the geology is highly fractured and landforms are in high relief. In addition, frequent earthquakes combined with heavy rainfall impose further stress to the earth's surface, with mass movements such as landslides, slumping, and mudflows occurring frequently.

Satellite remote sensing platforms that are currently providing image data include Landsat-7, Terra, Aqua, Envisat, SPOT, NOAA, ERS, RADARSAT, IRS, the Japanese ADEOS-2, Meteosat and other geostationary meteorological satellite systems, and high-resolution commercial systems such as IKONOS and Quickbird, with 1 m or less spatial resolution. In addition, NASA's earth observing-1 carries an imaging spectrometer, Hyperion, capable of resolving 220 spectral bands (from 0.4 to 2.5 μm) with a 30 m spatial resolution. The instrument images a 7.5 km by 100 km land area per image. Experience gained with airborne imaging spectrometers helps researchers to understand the problems of handling such large data volumes. Potential technical problems include the development of methods of combining multi-source (multi-sensor) data, handling large volumes of high-resolution data, and selecting the optimum combination of bands to use for a particular application.

Different approaches of remotely sensing data exist, in-cluding aerial photography, optical satellites, synthetic aperture radar imagery, and topographic data acquisition. They can all be used for landslide inventory (Barlow et al., 2003; Chang et al., 2010; Delacourt et al., 2003; Liu et al., 2009; NFA, 2008). Aerial pho-tography has long been extensively used to characterize land-slides and to produce landslide inventory maps, particularly because of their stereo-viewing capability and high spatial resolution (Mantovani et al., 1996). Satellite imagery can also be used to extract information of geological features, geomorphology, land use, hydrology, and so on. However, most landslide detection is based chiefly on spectral features of remotely sensed images other than topographic features. Because the spectral features of buildings and roads are similar to those of landslides, serious misjudgments can occur (Parise, 2001).

2. Methodology

This study selects the 20 km long Tengjhih Forest Road which is the active region of geologic hazard from Liouguei District to Tengjhih National Forest Recreation Area as the study area. The region was damaged by Typhoon Mindulle in 2004, Typhoon Haitang in 2005, Typhoon Kalmaegi in 2008 and Typhoon Morakot in 2009. However, the slate gravity deformation has actually existed at 18K to 19K of Tengjhih Forest Road for ten years, and the triggering factors, such as heavy rainfall, cause massive landslide. If the symptom and region of probable slide can be detected before the triggering factors cause disasters by means of the expected outcome of this study, the early warning technology for soil and water conservation will be enhanced greatly.

2.1. Used Satellite Data

The Formosa II satellite with a high resolution of 2 meter panchromatic data and 8 meter multispectral satellite image data, was successfully launched on May 21, 2004. The main mission of FORMOSAT-2 is to conduct remote sensing imaging over Taiwan and on terrestrial and oceanic regions of the entire earth. Its applications cover land use and change, agriculture, forestry, planning, environmental monitoring, disaster assessment and scientific education. The specification of the Formosa II lists as follows (Astrium webpage, 2014):

Table 1. Sensor specifications for the FORMOSAT-2 satellite

Track Altitude	891 km (AGL), Earth observation satellite
Revisit Interval	Daily
Resolution	• B&W: 2 m • Color: 2 m (merge) • Multispectral (R, G, B, NIR): 8 m
Spectral Bands	• P: 0.45 - 0.90 µm (Panchromatic) • B1: 0.45 - 0.52 µm (Blue)
	• B2: 0.52 - 0.60 µm (Green) • B3: 0.63 - 0.69 µm (Red) • B4: 0.76 - 0.90 µm (Near-infrared)
Sensor Footprint	24 km x 24 km

2.2. Change Analysis for the Landslide Vulnerability

Because newly formed landslides are mostly bare ground, their spectral reflectance curve becomes changed than before. Vegetation indices can be calculated by multispectral satellite images to explore the spectral characteristics of landslides. Among more than 20 types of vegetation indices, a standardized vegetation index called the Normalized Vegetation Index (NDVI) is the most commonly used indicator for surface biomass cover. The NDVI calculation formula is as follows:

$$NDVI = \frac{NIR - R}{NIR + R}, \qquad (1)$$

where NIR and R mean the digital number on the near-infrared band and one on the red band, respectively.

Use Compute Difference Map to produce an ENVI classification image characterizing the differences between any pair of initial state and final state images. The input images may be single-band images of any data type. The difference is computed by subtracting the initial state image from the final state image (that is, final - initial), and the classes are defined by change thresholds. A positive change identifies pixels that became brighter (final state brightness was greater than the initial state brightness), while a negative change identifies pixels that became dimmer (final state brightness was less than initial state brightness).

2.3. Dedicated 3-D Digital Platform in Cloud

Finally, this work will present the test results on the 3D dynamic digital earth platform by real-time on-line release, a new disaster analysis interpretation and release procedure is completed, increasing the

effectiveness of disaster prevention and protection. The 3D platform developed by Lidar Technology Co., Ltd., the major functions are spatial information value adding, release and browse. The purpose is to construct topic map faster, more intelligently and more simply, so as to enhance the information conveying capacity. Users can add various spatial information (vector, grid, 3D object data) to the platform, with the existing base maps and landforms of platform for value adding. The major functions include circling, labeling, enhancing the vision of key region, adding GPS trajectory, video, picture and text for assistant description, release to network after value adding, the user can implement 2D/3D viewing angle switching on the platform easily, clicking the conveyed spatial information subject.

3. Results and Discussion

After preprocessing of satellite images, including radiance calibration and geometric calibration, the cut multispectral image on 2007 for the study area is shown as Figure 1. For the limitation of paper pages, other conducted satellite images taken on 2008 to 2015 did not show here. Owing to worse quality of image on 2009, so it was not used in the experiment.

Figure 1. FORMOSAT-2 satellite image on 2007

Next the near-infrared and red band in each used multispectral images were used to generate NDVI image follow the equation (1), respectively. The derived NDVI image on 2010 is shown as Figure 2. In this figure, the pixels in green color represent positive NDVI value,

and ones in brown color mean negative NDVI value. Then two NDVI images for different time were used in the change detection. A threshold value of ±0.15 had been used to identify positive, no, and negative change. The change results between 2007 and 2010 had been demonstrated in Figure 3 and Figure 4. The pixels in red color represent negative change, which mean vegetation cover in the initial state change to bare land. The blue ones mean positive change, and ones in white are no changed. We can easily recognized continuously expanding trends for the landslide according to the time-series land cover change. It also can be observed the active area can be separated into two sub-areas, mean eastern part and western one.
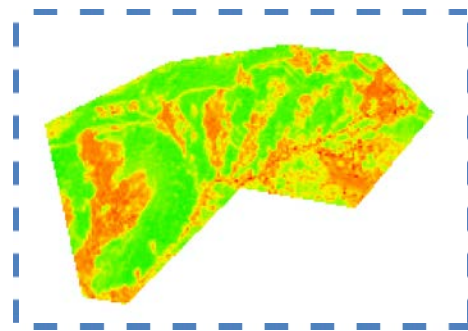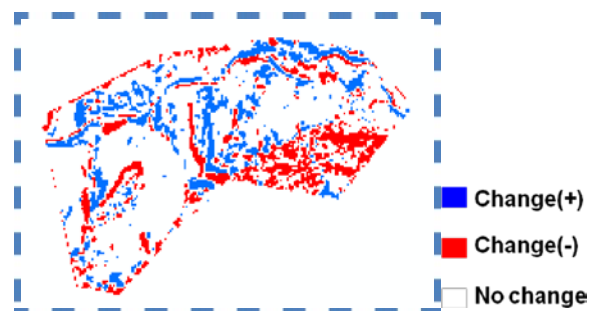

Figure 2. NDVI image on 2010

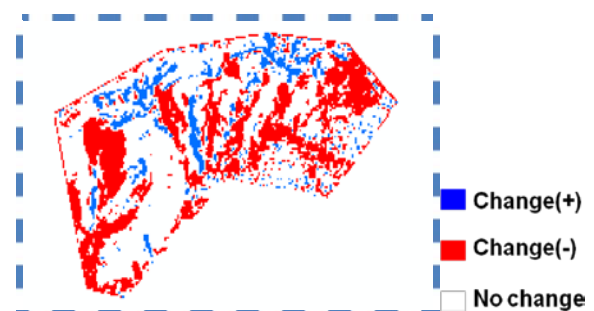**Figure 3. Land cover change map during 2007 and 2008**

Figure 4. Land cover change map during 2008 and 2010

Finally, the multi-temporal change results had been published on a dedicated 3-D digital platform shown as Figure 5 and Figure 6. The following analysis of landslide vulnerability and monitoring planning can be performed under the help of this digital platform.
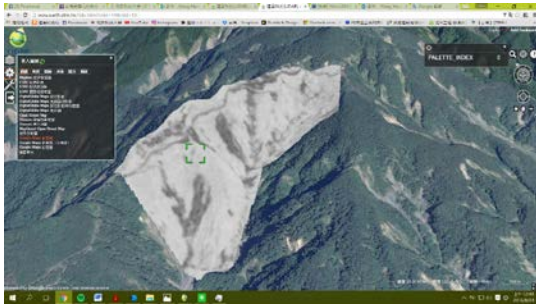

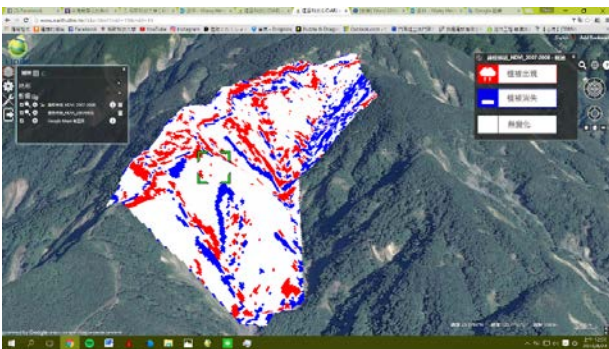**Figure 5. NDVI result 2007 published on the dedicated 3-D platform**

Figure 6. Change result published on the dedicated 3-D platform during 2007 and 2008

3. Conclusions and Suggestions

The experimental results indicate that continuously expanding trends for the landslide for the study area and two active sub-area can be inferred. However, further field validation is necessary. Moreover, the multi-temporal change results published on a dedicated 3-D digital platform are indeed helpful for the landslide vulnerability and monitoring planning.

Acknowledgement

References

Astrium webpage, 2014. Formosat II product sheet, Access date : 15 March. URL: http://www.astrium-geo.com/en/160-formosat-2

Barlow, J., Martin Y., and Franklin S. E., 2003. *Detecting translational landslide scars using segmentation of Landsat ETM+ and DEM data in the northern Cascade Mountains, British Columbia. Can. J. Remote Sensing*, Vol.29, No.4, 510–517.

Chang, K. T., Liu, J. K., Chang, Y. M., and Kao, C. S., (2010). An accuracy comparison for the landslide inventory with the BPNN and SVM methods, *Gi4DM 2010*, Turino, Italy.

Delacourt, C., Allemand, P., Squarzoni, C., Picard, F., Raucoules, D., and Carnec, C., 2003. Potential and limitation of ERS-Differential SAR interferometry for landslide studies in the French Alps and Pyrenees, Proc. Of FRINGE.

Liu, J. K., Chang, K. T., Rau, J. Y., Hsu, W. C., Liao, Z. Y., Lau, C. C., and Shih, T. Y., 2009. *The Geomorphometry of Rainfall-Induced Landslides in Taiwan Obtained by Airborne Lidar and Digital Photography*, *Geoscience and Remote Sensing*, In-Tech, Inc.

Mantovani, F., Soeters, R., and Van, C.J., 1996. *Remote sensing techniques for landslide studies and hazard zonation in Europe*, *Geomorphology*, Vol.15, 213-225.

NFA, 2008. *Historical records of natural disasters of Taiwan from 1958 to 2007*, National Fire Agency, Ministry of the Interior, Access date : 31 December. URL: http://www.nfa.gov.tw/Show.aspx?MID=97&UID=827&PID=97.

Parise, M., 2001. *Landslide mapping techniques and their use in the assessment of the landslide hazard*, *Physics and Chemistry of the Earth*, Vol.26, No.9, 697-703, doi:10.1016/S1464-1917(01)00069-1.